Department of AERONAUTICS and ASTRONAUTICS
STANFORD UNIVERSITY

B. T. ALLIGOOD
J. B. KYSER
D. W. TSAO

A TRAVERSING PROBE FOR PITOT-PRESSURE MAPPING IN A HYPERSONIC TUNNEL

SEPTEMBER
1963

Technical Report No. 1
Prepared as a part of Project DEFENDER,
Under Contract Nonr-225 (65)
Task NR 061-133

SUDAER
NO. 170

Department of Aeronautics and Astronautics
Stanford University
Stanford, California

A TRAVERSING PROBE FOR PITOT-PRESSURE MAPPING IN A HYPERVELOCITY TUNNEL

by

B. T. Alligood,
J. B. Kyser and D. W. Tsao

SUDAER No. 170
September 1963

This work has been sponsored by the
Advanced Research Projects Agency (Ballistic Missile Defense Office)
and technically administered by the Fluid Dynamics Branch
of the Office of Naval Research

ABSTRACT

An account is given of the design, construction, and operation of a multi-probed axially traversing pitot-pressure rake, which was designed to measure wake pressure profiles behind models in the Stanford spark-heated wind tunnel. Criteria considered in the design of the traversing probe are discussed. The mechanical operation of the probe during bench tests and during initial experiments in the tunnel is described, and velocity-time diagrams are given. Examples of the pressure data that have been taken in the wake behind a cylindrical model are presented and discussed briefly.

TABLE OF CONTENTS

LIST OF ILLUSTRATIONS

ACKNOWLEDGEMENT

The work described in this report was part of a general investigation conducted by the Department of Aeronautics and Astronautics at Stanford sponsored by the Advanced Research Agency (Ballistic Missile Defense Office) and technically administered by the Fluid Dynamics Branch of the Office of Naval Research, Contract No. Nonr-225(65).

The authors wish to express their appreciation to Professor Walter G. Vincenti for his scientific guidance and encouragement during the course of this investigation. They wish also to thank Messrs. Vadim Matzkevitch and Arthur Tonella for their assistance during the construction of the apparatus.

1. INTRODUCTION

The Stanford spark-heated wind tunnel is a high-enthalpy facility of the so-called "hotshot" type. The major portion of the work which is being done with the tunnel at this time is directed toward the study of hypersonic wakes behind models. To assist in the computation of wake density profiles it was necessary to construct instrumentation capable of making pitot-pressure surveys in the wake. Although pitot-pressure surveys can be made with a fixed multi-probed pressure rake, each tunnel run would yield the pressure profile at only one axial station in the wake. Consequently, investigation of an appreciable portion of the wake would require a large number of runs and it is questionable whether tunnel conditions could be precisely repeated from one run to the next.

Pravitz, of Boeing Aircraft Corporation, has used an axially translating pressure probe to investigate axial pressure gradients along the centerline of Boeing's spark-heated tunnel (Ref. 1). As an extension of the technique, a traversing multi-probed rake has been constructed for use in wake investigations at Stanford. Figure 1 is a photograph of the completed probe, and Fig. 2 shows the probe mounted in the tunnel. The pressure rake, which houses 8 wafer-type pressure transducers, is mounted on a spring-driven telescoping tube. The operating characteristics of the probe permit the mapping, during a single run, of the pressure in a planar portion of the wake 3.5 inches high and 8 inches long. This report describes the design, construction, and operation of this axially traversing probe. The analysis of the data from the initial runs has not yet been completed and is not discussed in this report. However, for illustration, some representative data from selected runs have been included.

2. GENERAL CONSIDERATIONS

The Stanford spark-heated wind tunnel, in which the traversing-probe experiments were conducted, is of the so-called "hotshot" type. The major components of the tunnel are an arc chamber (or reservoir), a hypersonic nozzle and test section, a vacuum tank, and a bank of capacitors for energy storage. The basic parameters of the Stanford tunnel are as follows:

Test-section diameter (at exit)	18.9 inches
Included cone angle of nozzle	8° 20'
Total energy storage of capacitor bank	200,000 joules
Free volume of arc chamber (can be varied by using different liners)	16 to 30 cubic inches

A detailed description of the tunnel and its operation is given in Ref. 2.

Tunnel operating characteristics, physical dimensions, and the number of available transducers and recording channels were considered in the preliminary design of the translating probe. The following design requirements were established:

(a) Sufficient space to house 8 pitot-pressure transducers;

(b) Minimum translational velocity of 30 fps;

(c) Completion of acceleration within 8 inches;

(d) Minimum acceleration-free travel of 8 inches;

(e) Completion of deceleration within 2 inches.

The number of transducers installed in the probe was limited primarily by the number of available recording channels. Although 12 channels are available, three channels are used for pressure transducers located elsewhere in the tunnel. One transducer is mounted in the reservoir, and the other two are mounted in the 1.0-inch-diameter cylinder which is used as a model for wake studies. The reservoir pressure and the pitot pressure at the model leading edge are used in calculating tunnel conditions. The model pitot pressure is also used as a normalizing reference pressure for the probe data.

At a velocity of 30 fps, the probe traverses the 8-inch test region in 22 milliseconds. Since the nominal run duration of the tunnel is 30 to 40 milliseconds, this velocity is sufficient for the probe to complete its traverse within the tunnel run time. Since total pressure in the test section decays with time, however, it would be desirable to increase the velocity of the probe to reduce variation of tunnel conditions during a run. The problem in increasing the probe velocity is that, if the same limitations are imposed on the probe's travel during acceleration, the forces on the transducers and wiring may become excessive.

The objective of the limitation on total travel was to reduce the overall length of the probe and to minimize the extension of the probe support into the diffuser section. Since the effect of a large blockage area on the tunnel's operation was unknown, an effort was made to keep the probe small.

With the basic requirements established, some of the general physical aspects of the design were then considered.

A spring system and a pneumatic system were each considered as a means of propelling the probe. A spring-driven system has the advantage of simplicity in design and construction and can be calibrated to yield any velocity up to its design velocity. Its major disadvantage is that, within the close confines of the tunnel, compressing the spring presents a problem. By placing all the valving and the air supply external to the tunnel, a pneumatic system could be designed that would require less tunnel space than a spring and trigger assembly. Such a system would also eliminate the problem of compressing a spring. Because of the difficult problems in design and construction of a pneumatic system, however, it was decided to adopt a spring-driven probe.

Methods of compressing the spring, and of triggering and stopping the probe were next considered. Preliminary estimates showed that a force of approximately 150 lbs would be necessary for compression of the spring. Loading the spring from the front of the probe by pushing the shaft of the pressure rake against it (see Fig. 4) is impractical

because of the large force involved. By mounting the spring inside a pipe, however, which was threaded to screw inside the rear of the probe housing, the spring could be compressed against the "cocked" rake shaft by screwing the pipe into the probe housing.

Sliding friction, impact against a crushable material, and compression of a spring were each considered as a means of stopping the probe at the end of its travel. To prevent damage to the probe, the deceleration loads had to be kept to a minimum. For a fixed stopping distance, minimum peak deceleration occurs with constant-force braking. Both a friction brake and a crushable material can be designed to give constant deceleration. The crushable material, however, requires replacement following each run. The spring was eliminated from consideration because it does not have the constant-force characteristic. Consideration of these factors led to the selection of a sliding-friction brake.

3. DESIGN AND CONSTRUCTION

3.1. Pressure Rake and Shaft

The design of the probe housing, spring system, and braking system is dependent on the total weight of the rake and the driven shaft. Any increase in the weight of the rake or the shaft requires a heavier spring and braking system, and may require strengthening of the housing. Consequently, the pressure rake was made as light as possible while still fulfilling strength requirements and providing the internal volume necessary for the transducers and associated wiring.

The pressure transducers are of the wafer type (Figs. 3 and 4, Ref. 3) and are 0.575 inches in diameter and 0.186 inches thick. The transducers and associated wiring require a space 4 inches wide, 2 inches long, and 0.5 inches deep. To save space and weight, and to simplify installation of the transducers, the rear member of the rake was designed to be used as an integral pressure manifold for the reference side of the transducers. This manifold is connected to the reference tank of the tunnel. The leading edge, which has pitot tubes of 0.040 inches inside diameter glued in place, was designed to be easily replaceable so that the pitot-orifice spacing could be varied. The entire pressure rake was constructed of aluminum and assembled with 2-56 machine screws. Except for the removable cover and leading edge, epoxy glue was used to strengthen and add rigidity to the rake.

The rake shaft is supported by Teflon bearings in the nose cone, and at the rear by slots in the outer casing in which the two flanges (or runners) ride. The bearing system is shown in Figs. 4 and 5. In addition, the runners engage the friction brake which stops the probe. From consideration of the total travel of the probe and the space required for the trigger assembly, it was determined that the rake shaft should be 34.0 inches long with the trailing edge of the 3.5-inch runners 4.0 inches from the rear of the shaft. An aluminum spacer bar of the same length and thickness as the runners was fitted inside the tubular shaft. The spacer bar, the runners, and the shaft were then joined together with epoxy glue and 1/8-inch steel rivets as shown

in Fig. 5. The tube was thus prevented from becoming crushed by the compression loads resulting from the braking process.

3.2. Spring Assembly

There are several theories in use for describing the motion of a mass driven by a compressed spring. The so-called massless-spring theory, based on static concepts, gives good results if the mass ratio is large, that is, if the driver mass M is large compared with the spring mass m. For other than large mass ratios, however, the mass of the spring cannot be neglected. An approximate solution based on the assumption of a concentrated spring mass improves the results for medium mass ratios. For small mass ratios neither theory is adequate.

Maier, in Ref. 4, analyzes the motion of a spring and mass system according to the so-called "surge-wave" theory. The equations derived by this theory predict the behavior of the spring and mass for low mass ratios. In particular, the surge-wave theory predicts an upper bound for the extension velocity that can be obtained with a compressed spring. Equations derived from this theory were used to design the traversing-probe spring.

Physical and functional requirements that were established for the probe spring are as follows:

(1) A maximum mean coil diameter of 1.0 inches;
(2) A maximum wire diameter of 0.180 inches;
(3) A deflection of the spring of between 4 and 6 inches;
(4) A maximum spring stress of 100,000 psi;
(5) Free length of the spring as short as design limits will allow.

The procedure used in designing the spring can be outlined as follows:

1. Choose suitable values for the following parameters:

S = stress
F = spring deflection
V_M = velocity of the driven mass
D = mean coil diameter

2. Calculate the "free spring velocity" u_i from the equation

$$u_i = 0.99\ S \sqrt{\frac{g}{2\gamma G}} \quad ,$$

where

g = gravitational constant

γ = specific weight of spring material

G = torsion modulus

This equation defines the velocity with which a spring, compressed such that its initial stress is S, will extend when suddenly released.

3. The velocity V_M of the driven mass M is given by the equation

$$V_M = u_i\{2 \exp[-\tfrac{1}{2} \exp(-2m/M)] - 1\}$$

which can be solved for the spring mass m.

4. The standard stress-deflection equation for compression springs is

$$S = \frac{FGd}{\pi D^2 N} \quad ,$$

where

d = spring wire diameter

N = number of active coils

This equation and the equation which defines the mass of the spring

$$m = \frac{\gamma \pi^2 d^2 DN}{4g}$$

can be solved together to determine the unknowns N and d.

5. The force P required to compress the spring is finally

$$P = \frac{Sd^3}{8D} \quad .$$

If the spring defined by the computations outlined above does not meet the desired physical specifications in some way, other parameters than those chosen can be fixed, and the spring redesigned.

The spring which is used in the probe was designed by the foregoing method based on a spring deflection F of 6 inches, a spring stress S of 100,000 psi, a coil diameter D of 1.0 inches, a velocity V_M of 35 fps, and a driven mass M corresponding to a weight of 1 lb. Because of subsequent modifications, the weight of the rake and shaft has been reduced slightly and a spring deflection of 4.25 inches now gives a velocity of 30 fps.

A 10-inch piece of 1.5-inch outside diameter threaded brass pipe was fitted at one end with a steel nut, as shown in Fig. 4. The spring was then placed inside the pipe, with one end attached to the steel nut by means of a 0.5-inch diameter rod which passes through the nut and spring. The rod, as shown in Fig. 4, also serves as a guide to keep the spring from buckling. A ball bearing between the spring rod assembly and the brass pipe keeps the spring and its guide stationary as the pipe is being screwed into the probe housing. The guide, which extends 0.25 inches beyond the end of the spring, moves inside the end of the rake shaft when the spring is compressed.

When mounted in the tunnel, the spring assembly on the end of the probe is difficult to reach, so that a special offset wrench was required. Loading the probe is easily done by means of this wrench.

3.3. Braking System

Two inches have been allowed for braking the rake to a stop at the end of its run. This is a compromise between keeping the deceleration forces on the rake to a minimum and obtaining data as near the model as possible. A constant braking force of 84 lbs is required to stop the rake in two inches from a velocity of 30 fps. On the basis of a friction coefficient of 0.20, the brake shoes must exert a normal force of 420 lbs against the probe.

To sustain the loads and to make the rubber braking pads easily accessible for inspection, these pads were glued into brass holders. These were then attached by steel pins to two steel plates mounted on the sides of the probe housing as shown in Fig. 4. The position of the

brass holders is adjustable by set screws; this varies the normal pressure against the shaft runners. The screws which attach the plates to the probe housing are loosened to release the pressure on the shaft after the probe is fired. Only the first 0.5 inch of the runners is tapered, so that after the shaft runners initially hit the brake, the force against the probe is essentially constant until the probe stops.

3.4. Probe Housing

Aluminum was used for the probe housing, except for a 24-inch steel section of the bottom cover which is welded to the strut. In essence, the probe housing is a square box constructed by joining 0.375-inch-thick bars, which form the sides, to the top and bottom covers which are made of channel aluminum. The square-box arrangement provides good accessibility to the moving parts and was simple to build.

Grooves for the runners on the shaft were milled into the aluminum bars on either side and lined with 0.035-inch-thick Teflon sheeting, which provides a low-friction bearing surface for the runners. Any excessive loose motion of the runners in the grooves is amplified at the rake, and the rake will not keep its position on the tunnel centerline as it travels toward the model. To prevent this, care was taken to maintain a close fit between the bearing surfaces.

The front bearing (see Fig. 4) consists of 3 pieces of Teflon rod mounted radially in the nose cone at 120° intervals so as to provide three contact points for the shaft to ride on. The set screws which hold the bearing rods in place can be adjusted to vary the clearance between the end of the rods and the rake shaft.

The rear end of the probe housing was bored out to provide clearance for the spring housing. A 2-inch-square brass block, threaded to receive the pipe with the spring enclosed, was bolted to the end as shown in Fig. 4.

3.5. Strut

The strut, in addition to providing a rigid support for the probe, must enclose the wiring with sufficient space for the motion of the

wiring as the probe is fired. An 18-inch-long slot for the wiring was cut in the bottom cover of the probe housing and the primary structural members of the strut, the steel bars (Fig. 4), were welded to the lower cover at the ends of the slot. The other ends of the bars were welded to a steel plug which fits into the lower access point on the tunnel. The sheet-steel covers add rigidity and prevent exposure of the wiring to the gas flow. One of the covers is welded in place; the other is attached by screws for access purposes.

Alignment of the probe relative to the tunnel centerline can be adjusted by means of the two main mounting bolts and the front and back screws shown in Fig. 4. No provision was made for changing the axial position of the probe.

3.6. Trigger Assembly

After consideration of several possible methods of triggering the probe, it was decided to build a trigger consisting of a rotating cam and sear actuated by an electrical solenoid (see Fig. 6). The mechanical advantage of this trigger is such that only a small force is required to actuate the sear. Even so, an excessively large linear solenoid would have been required since this type of solenoid develops its minimum force at the beginning of its stroke. A Ledex 5E 25° rotary solenoid, designed to deliver constant force during its entire stroke, was used; this resulted in a reduction in the size of the trigger assembly.

The bearing surfaces between the cam and the sear were made of hardened tool steel because of the high bearing loads. The alignment between the pin-jointed sear and cam is critical; therefore, considerable care was taken in the design and construction of these members. If misalignment occurs, the trigger could either release spontaneously or the force required to release the sear could be greatly increased. As a safety factor, a solenoid larger than actually necessary was used. An advantageous side effect has been that any variation in the time between the application of power to the solenoid and the release of the trigger has been virtually eliminated.

3.7. Position Transducer

As the rake moves toward the model, each pressure transducer continuously measures the pitot pressure, which is recorded by means of a CEC 26-channel oscillograph. By feeding the output from a rake-position transducer to one of the galvanometers of the oscillograph, the relation between rake position and the pressure traces is established.

In the evaluation of several types of position transducers, primary consideration was given to the selection of a transducer which would neither add weight to the shaft nor restrict its motion. The photocell system shown in Figs. 7 and 8 was selected for this reason. It is simple in operation, and requires only that the shaft have narrow light reflecting strips at graduated intervals.

A Texas Instruments H-35 photo-conductive cell is mounted, at a 45° angle to the probe axis, inside an aluminum block which is attached to the front lower cover of the probe housing. Also at 45° to the probe (90° from the photocell) is a 27.5-volt aircraft instrument light. The photocell is connected in series with a variable resistance and a 45-volt battery.

In operation, narrow reflection (target) strips, at graduated intervals on the shaft, reflect the light beam onto the photocell lens whenever one of these strips passes through the beam. The drop in resistance of the photocell causes the voltage across the series resistance to change. This signal is then recorded by means of either an oscilloscope or the CEC oscillograph. The magnitude of the output signal can be changed either by varying the applied voltage to the photocell or by changing the series resistance.

3.8. Probe Triggering Circuit

The average elapsed time between the initiation of the electrical discharge in the arc chamber and the establishment of quasi-steady flow in the test section is approximately 10 milliseconds. On the other hand, calculations (and bench tests) showed that the elapsed time from application of power to the trigger solenoid until the rake reaches a

velocity of 30 fps is approximately 30 milliseconds. This means that the probe must be fired prior to firing the tunnel.

Figure 9 shows the circuit which was devised to give the required time delay. Depressing the start switch applies power to relay (3) which closes and completes the 90-volt dc circuit to fire the probe. Firing of the tunnel is delayed by relays (1) and (2), which must close before the electrical discharge in the arc chamber can occur.

To prevent overheating and possible damage to the Ledex solenoid, relay (4), which is normally closed, breaks the 90-volt dc circuit when switch (a) is closed. The 0.05-mmf capacitor prevents arcing between the contacts when the probe is fired.

4. OPERATION AND RESULTS

4.1. Bench Tests

Prior to mounting in the tunnel, the probe was fired a number of times to test its mechanical operation. The first test run was made with the spring only partially deflected; this gave the rake a velocity of 20 fps. Following the successful completion of this run, the deflection of the spring was increased for successive runs, until the rake velocity reached 38 fps.

To see whether the rake was being subjected to high peak forces during the deceleration runout, target strips at 1/4 inch intervals were painted on the portion of the shaft which passes the photocell after the shaft runners initially hit the brake. The deceleration forces which act upon the rake while braking to a stop could then be deduced from the photocell output.

Figure 10 is an example of the photocell output from a test run during which the velocity of the rake was 31 fps. Evaluation of this data and the data from other similar runs showed that the deceleration force from braking is essentially constant.

For different runs with the same spring deflection, the bench tests showed that the rake velocity was repeatable, at least to within the accuracy to which the oscilloscope trace could be read. It is important that the velocity be repeatable to insure that, during actual runs with the probe in the tunnel, the rake will traverse the test region within the tunnel run time. It is also important that the "constant velocity" portion of the rake's travel actually be free from any appreciable deceleration in order to avoid possible effects on the output from the pressure transducers. Figure 11, a plot of rake position versus time, as made from the oscilloscope photocell trace, together with similar records verify that this is actually the case.

The series of bench runs did not reveal any serious flaws in the probe's operation, nor did any structural failures occur. The probe was therefore installed in the tunnel.

4.2. Tunnel Runs

The analysis of the data from the experiments with the probe in the Stanford tunnel has not been completed and therefore cannot be discussed in detail here. To illustrate the data which is being obtained with the traversing probe, however, and to point out its capabilities in making pressure measurements over a large flow field, three representative sets of data are shown in Figs. 12 through 22.

The oscillograph output from run A, a run made with no flow in the tunnel, is shown in Fig. 12. This was a run made to determine the effects on the pressure transducers' output of acceleration forces as the probe is fired, and of electrical noise induced by the probe trigger circuit or by the motion of the transducer wiring as the rake traverses down the tunnel. The letters on the pressure traces correspond to the pitot-probe spacing as shown in Fig. 5. The pressure transducers were calibrated and the attenuation of the carrier amplifiers adjusted as for a normal run. The usual practice for each run was to try to adjust the sensitivity to one psi per inch of trace deflection. Because of the amplifier design, however, sensitivities of output traces vary from 0.75 to 1.25 psi per inch of trace deflection.

There is little evidence of adverse effects from the acceleration forces at the beginning of the rake's motion. As expected, the transducers are affected to a greater extent when braking begins. Even under the high inertia forces which are encountered by the transducers as a result of the braking action, however, the noise level of the pressure traces does not become excessive. The probable reason that the transducers are relatively unaffected by acceleration forces is that they are mounted in the rake so that their diaphrams are parallel to the direction of motion.

The signal which is apparent on each of the pressure traces just before the probe starts moving was caused by electrical pickup from the

trigger solenoid. It has since been eliminated by completely shielding all of the transducer wiring.

The photocell output was recorded both by the CEC oscillograph and by an oscilloscope camera. The oscilloscope record for run A is shown in Fig. 13. Figure 14 is a time-distance plot of the photocell data. Zero time in this plot is the time when the first target, which is 0.05 inches from the photocell beam when the probe is in the cocked position, passed the photocell. The measured velocity which the rake attained during the run was 27 fps.

The oscillograph record from run B is shown in Fig. 15. This run was made with flow in the tunnel but without the cylindrical model installed so that the data could be compared with pitot-pressure data from earlier experiments made with stationary probes in the otherwise empty test section. This was the first run in which the tunnel and probe were fired together, and as can be seen, the probe was fired approximately 5 milliseconds late. With the model installed, late firing limits the region covered during the run, and data are not obtained close behind the model. The oscilloscope data and the time-distance plot are shown in Figs. 16 and 17. The velocity during this run was 28 fps.

Figure 18 shows the measured pitot pressure plotted as a function of time, where zero time is the time when the electrical discharge occurred in the arc chamber. The dotted portion of these curves is the pressure measured during the transient starting process of the tunnel. The beginning of quasi-steady flow is approximately at the point where the solid lines start.

The data from run C (see Figs. 19, 20, 21, and 22) are representative of the data obtained from runs with the one-inch cylindrical model mounted in the tunnel. The output traces from the two pitot-pressure transducers which are mounted in the model and the arc-chamber pressure trace are also shown on the oscillograph record (Fig. 19). The average of the data from the two transducers in the model was used to normalize the pitot pressures as measured by the traversing rake. The timing of the probe's firing during this run is considered optimum.

Figure 22, which is based on the data of Fig. 19, is a non-dimensional plot of the distribution of pitot pressure at a number of positions downstream of the model. In this plot y/d refers to the transverse (vertical) pitot-orifice position relative to the center of the rake divided by the model diameter (1 inch), and x/d refers to the axial distance from the pitot probe to the model centerline divided by the model diameter. Pressure profiles behind the model are shown at one-inch increments from $(x/d) = 4$ to $(x/d) = 13$ From this plot the decrease in the width of the wake is quite apparent as the rake approaches the model; it can be seen also that the wake center and the rake center did not coincide exactly. The profile at $(x/d) = 4$ gives evidence of the neck of the wake. The profile at this particular station has been verified by other runs with the probe traversing and by runs with the probe fixed.

5. CONCLUDING REMARKS

The axially traversing probe which has been built can effectively map the pitot-pressure distribution over a large flow field during a single tunnel run. It has several advantages over the use of fixed probes. Fewer runs are required to obtain a given amount of data; this reduces the uncertainty that results from the lack of precise repeatability of tunnel conditions from one run to the next.

The probe will operate satisfactorily up to a velocity of 38 fps. At a velocity of 30 fps, which is sufficient for runs in the Stanford hotshot tunnel, the rake requires 4.2 inches for acceleration and 1.8 inches for deceleration. There are thus 10 inches of constant-velocity travel in which to take data. It is probable, however, because of the negligible effect of acceleration forces on the transducers, that the data are actually reliable over a larger distance than this.

The data which have been obtained thus far with the traversing probe must be further analyzed and compared with other experimental and theoretical results before being accepted as valid. There is, in particular, a question concerning the possible effect of the response time of the transducers which has not been investigated. The pressure profiles which have been obtained must also be confirmed by increasing the number of data points. When analysis of the present data is completed, an investigation of the response time of the overall probe-amplifier-recorder system will be made. Following this, the pitot-pressure survey of the cylinder wake will be extended with the aid of several different rake configurations.

REFERENCES

1. Pravitz, J.E.: Axial Gradients in the Boeing Hotshot by Translating Probe Measurements. Paper presented at the 18th Semi-Annual Meeting of the Supersonic Tunnel Association, October 1962.

2. Karamcheti, K., Vali, W., and Vincenti, W. G.: Initial Experience in the Stanford Spark-Heated Hypervelocity Wind Tunnel. SUDAER No. 100, Department of Aeronautical Engineering, Stanford University, Stanford, California, January 1961.

3. Smotherman, W. E.: A Miniature Wafer-Style Pressure Transducer, AEDC-TR-60-11, Arnold Engineering and Development Center, October 1960.

4. Chironis, N.: Spring Design and Application, McGraw-Hill Publishing Company, 1961.

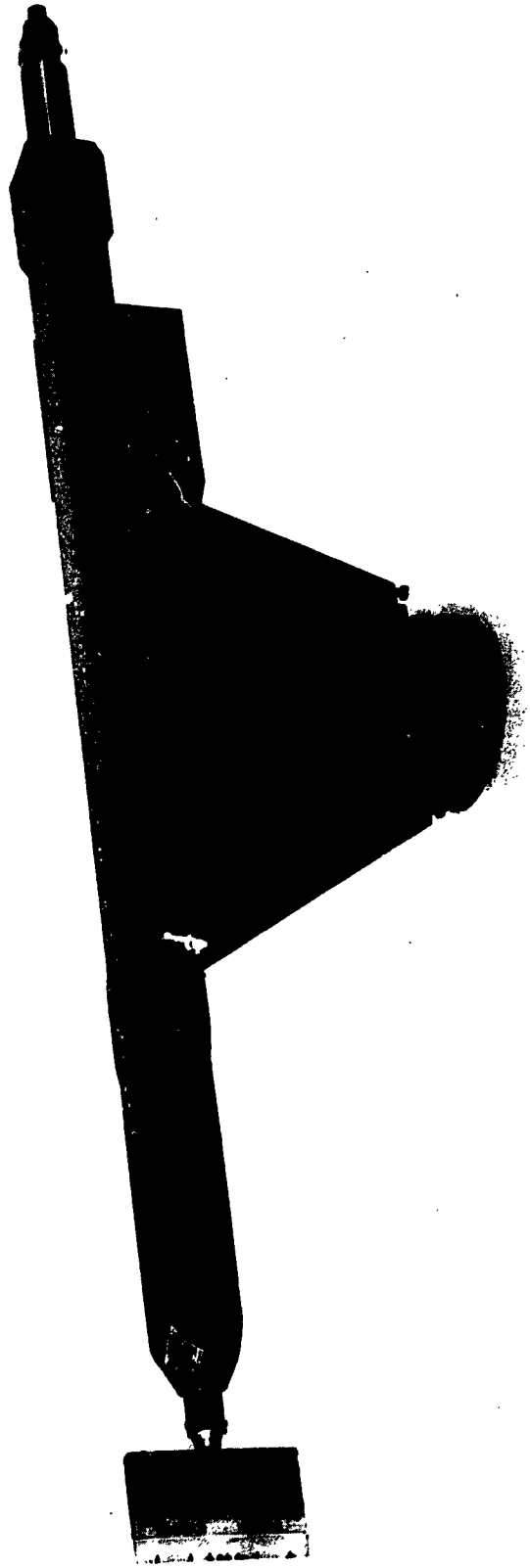

FIG. 1. AXIALLY TRAVERSING PROBE.

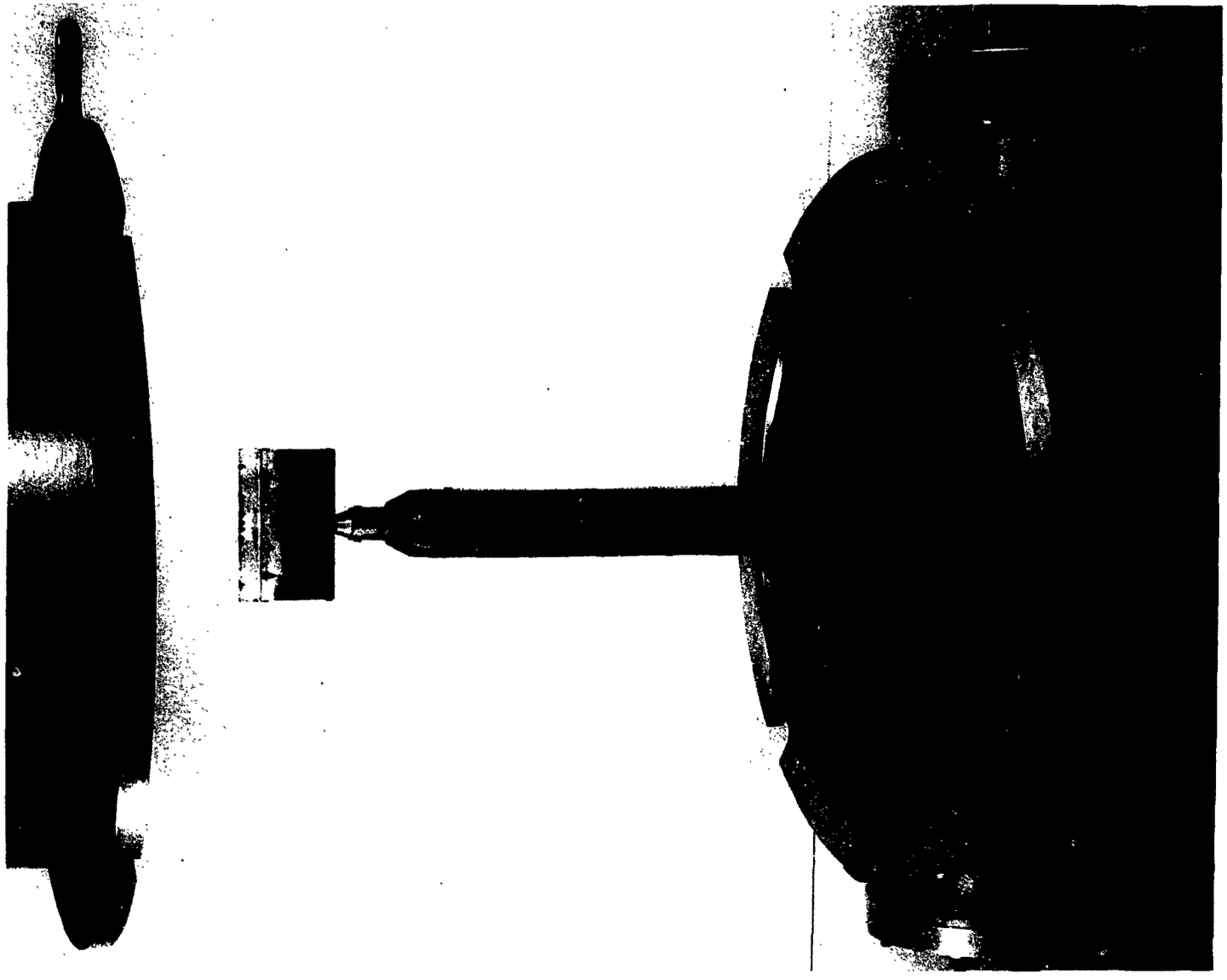

FIG. 2. AXIALLY TRAVERSING PROBE MOUNTED IN TUNNEL.

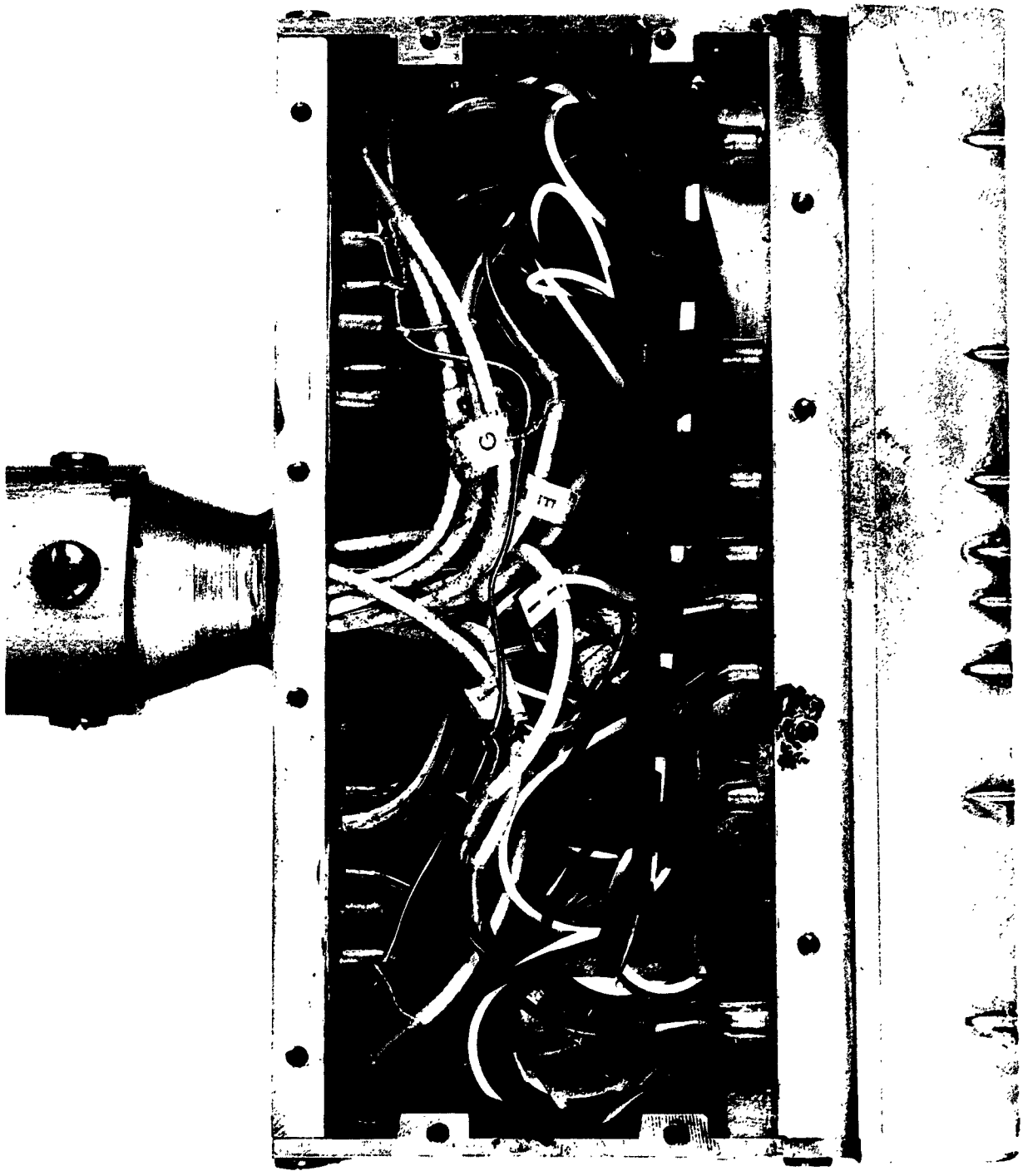

FIG. 3. PITOT-PRESSURE RAKE.

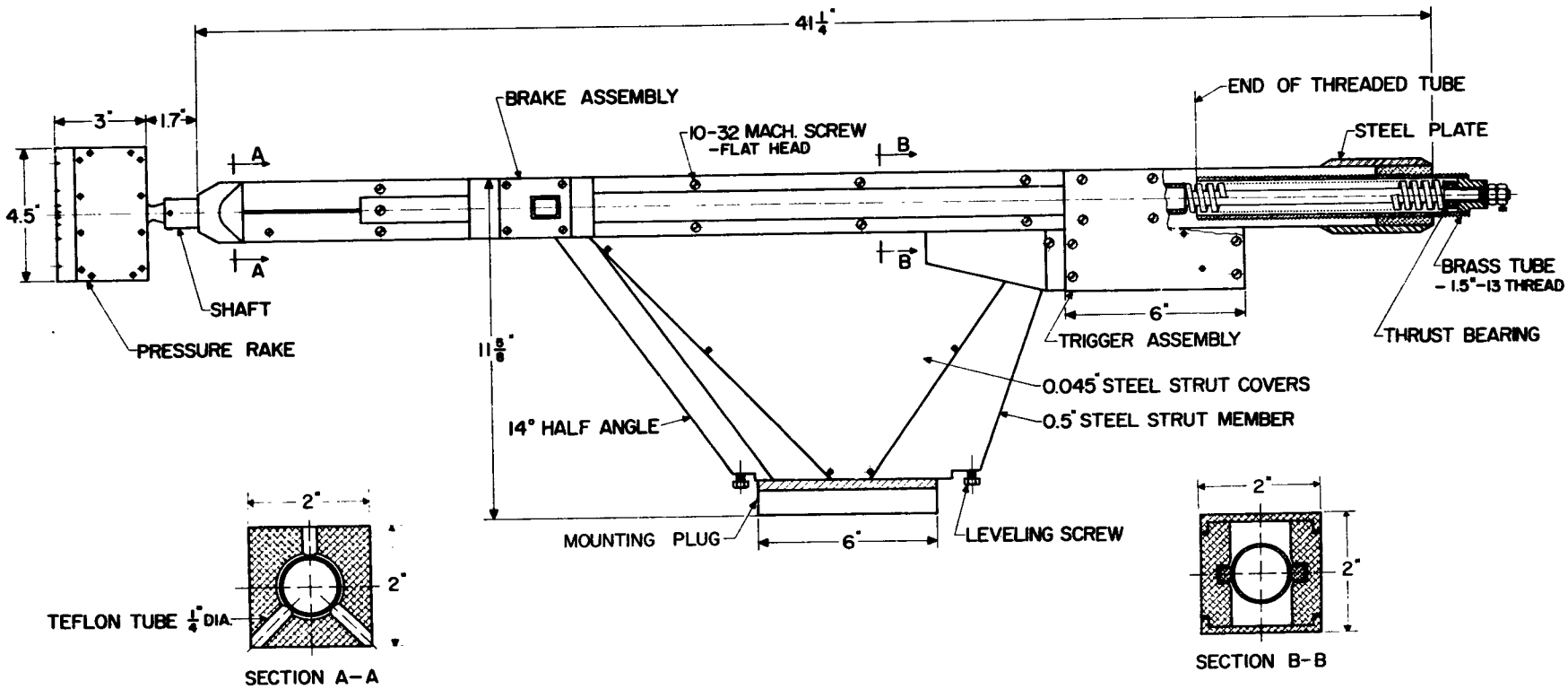

FIG. 4. AXIALLY TRAVERSING PROBE AND MOUNTING STRUT.

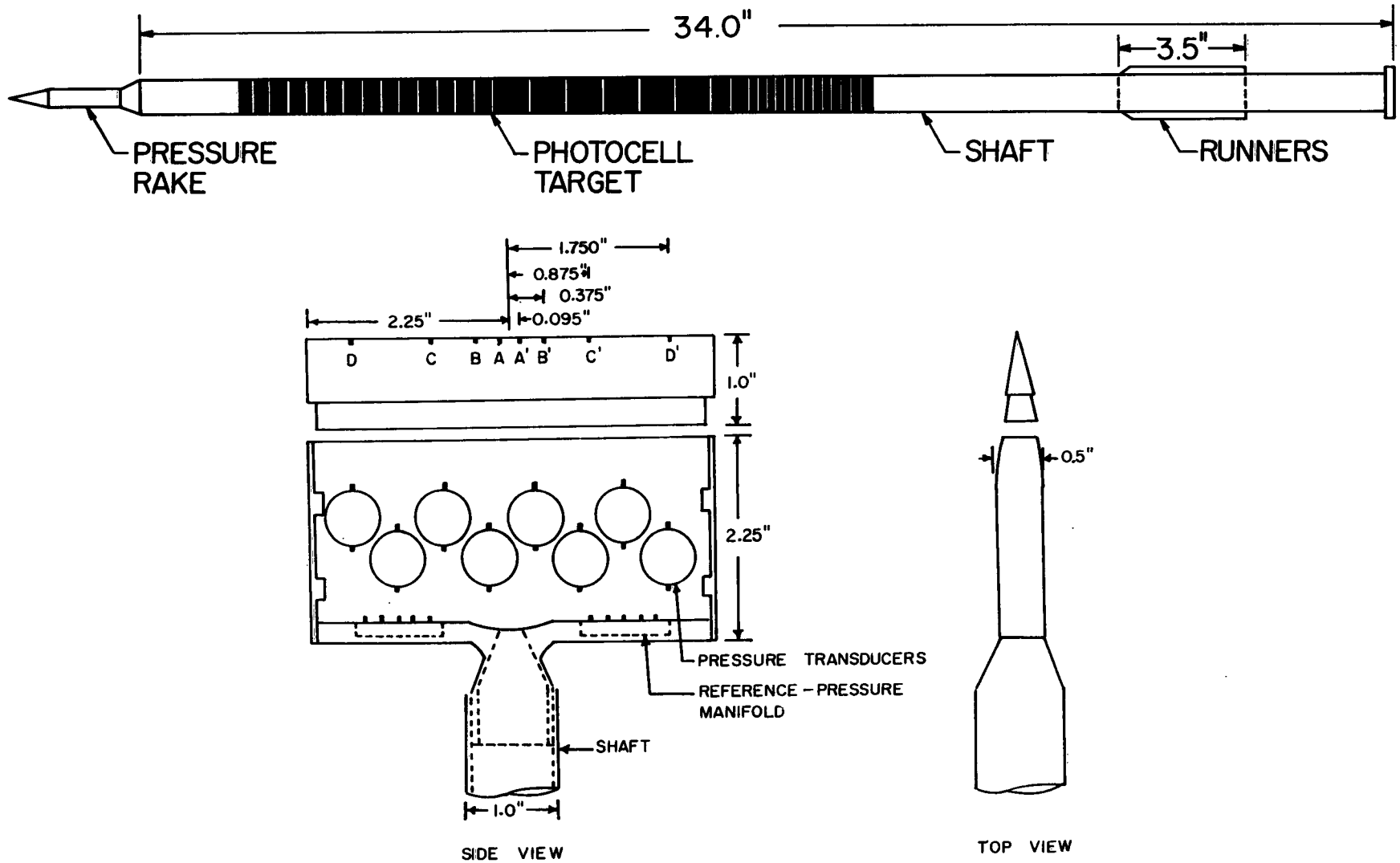

FIG. 5. PRESSURE RAKE AND SHAFT.

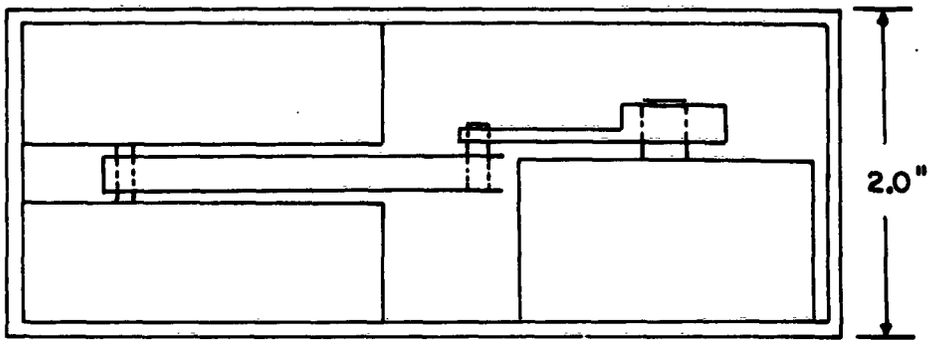

TOP VIEW

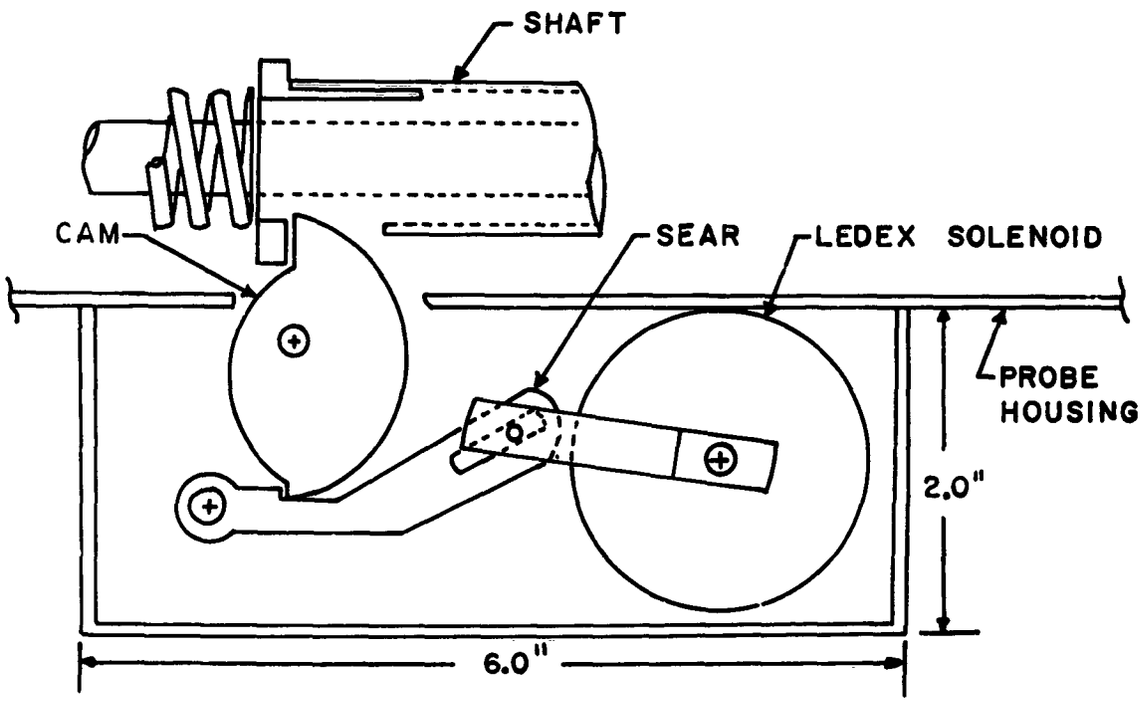

SIDE VIEW

FIG. 6. TRIGGER ASSEMBLY.

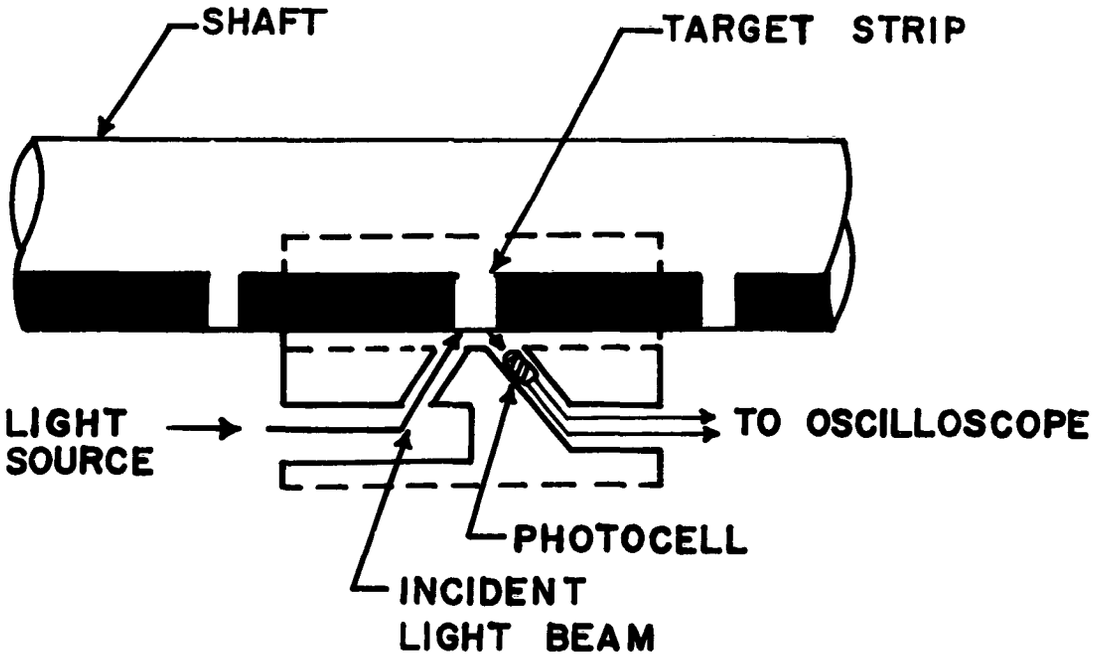

FIG. 7. SCHEMATIC DRAWING OF PHOTOCELL MOUNTING.

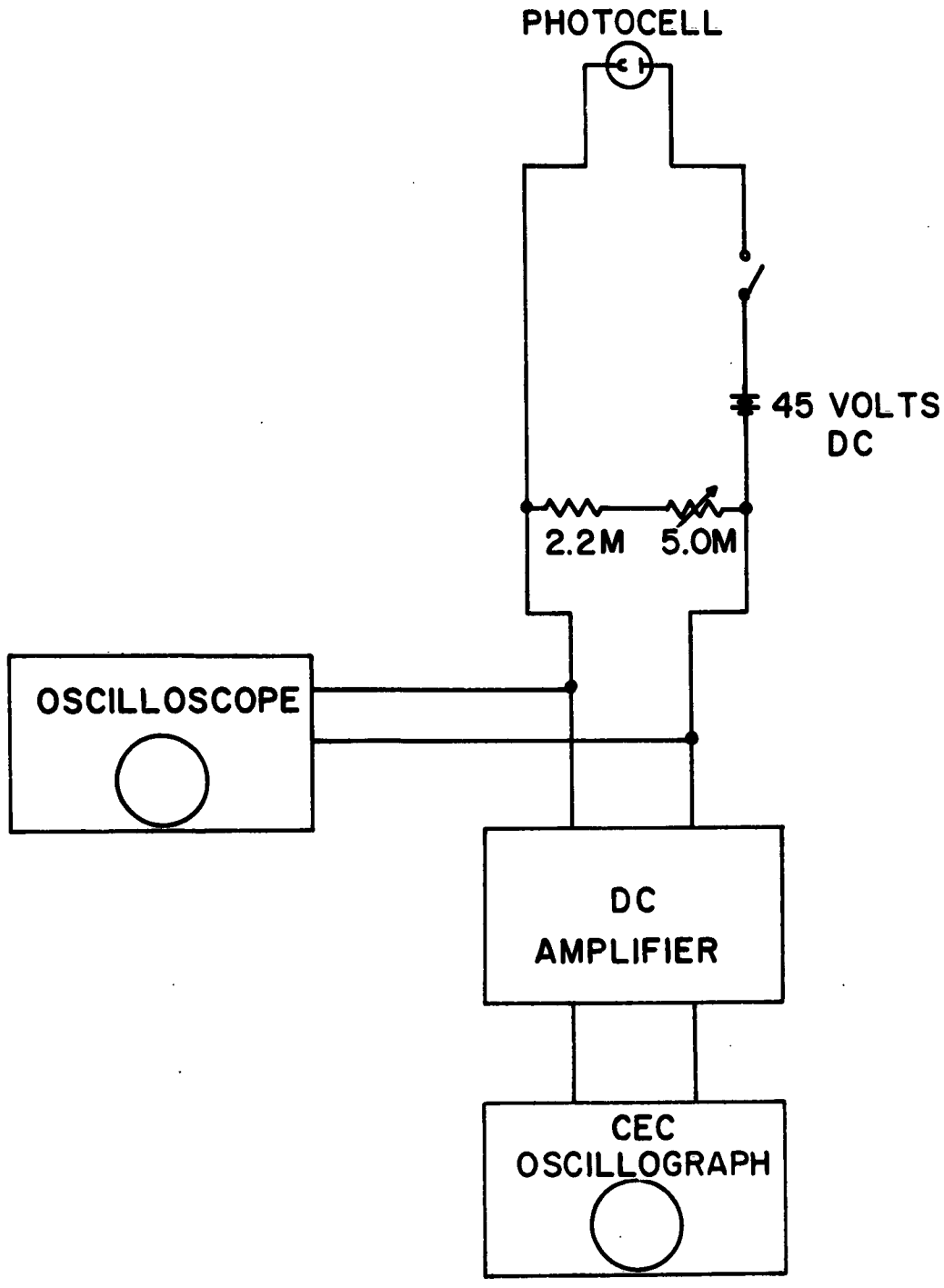

FIG. 8. PHOTOCELL CIRCUIT.

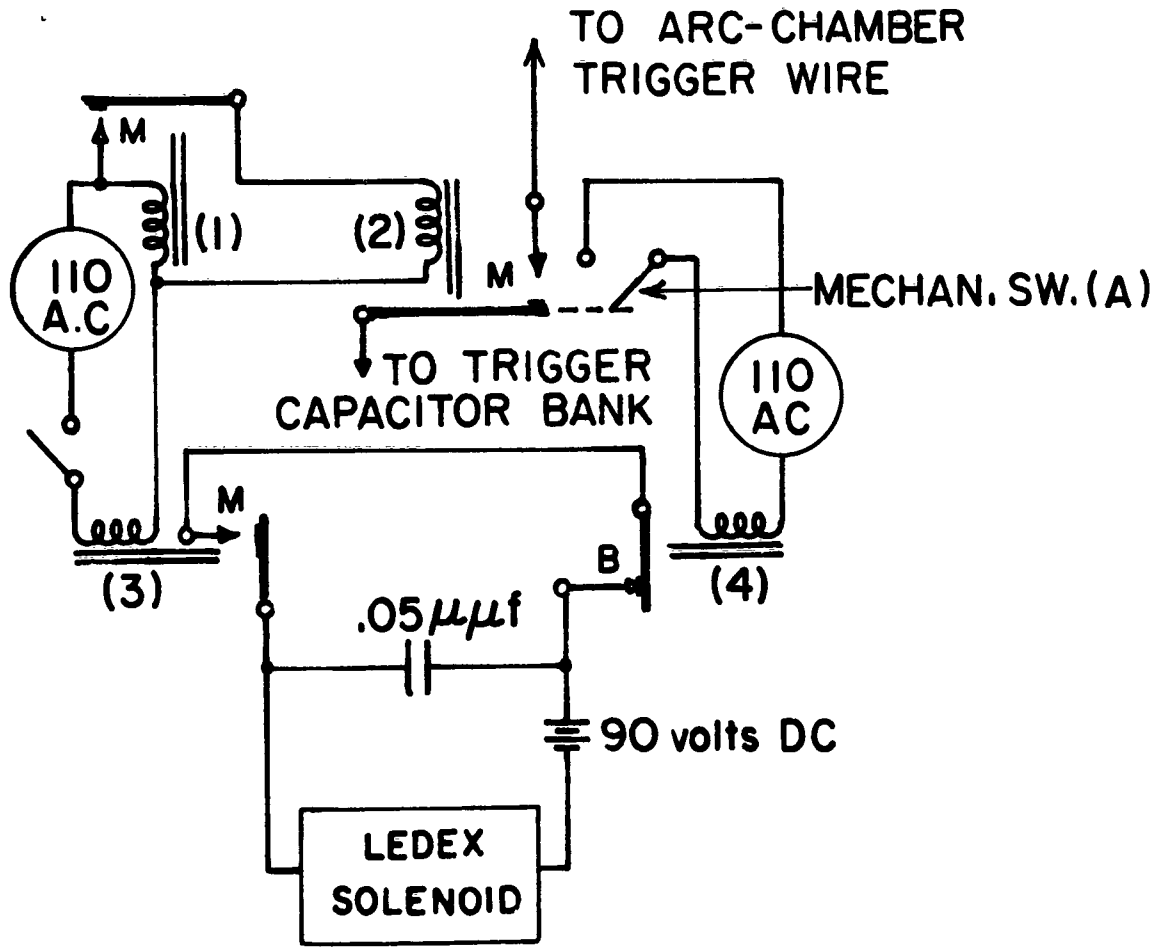

FIG. 9. TRIGGERING CIRCUIT.

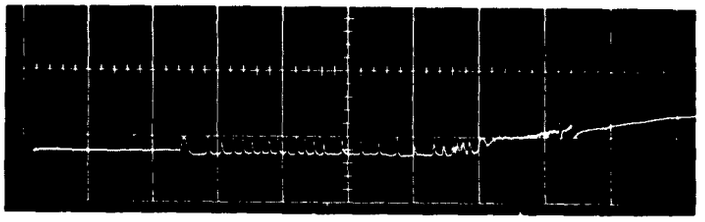

FIG. 10. OSCILLOSCOPE TRACE OF PHOTOCELL OUTPUT.
TIME SCALE: 10 MILLISEC/CM.

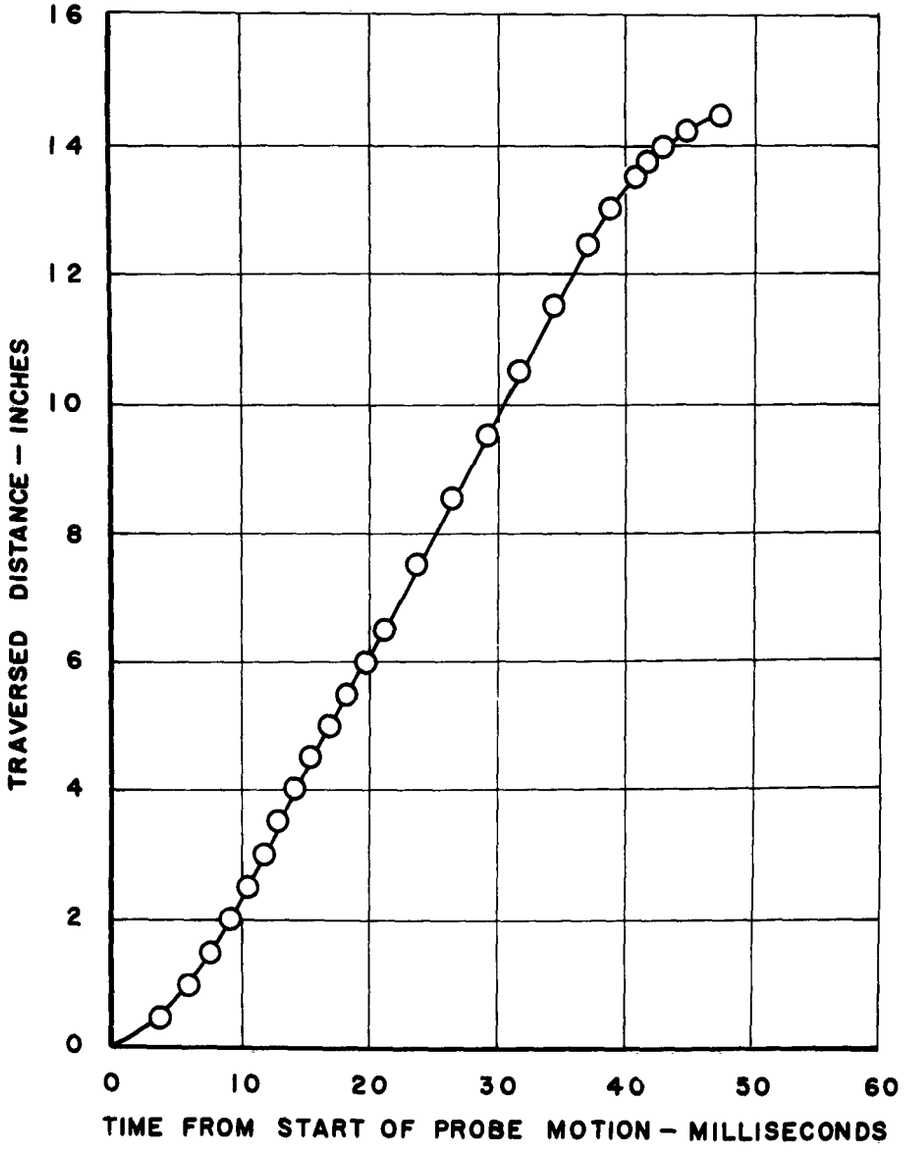

FIG. 11. TIME HISTORY OF POSITION OF PITOT-PRESSURE RAKE.

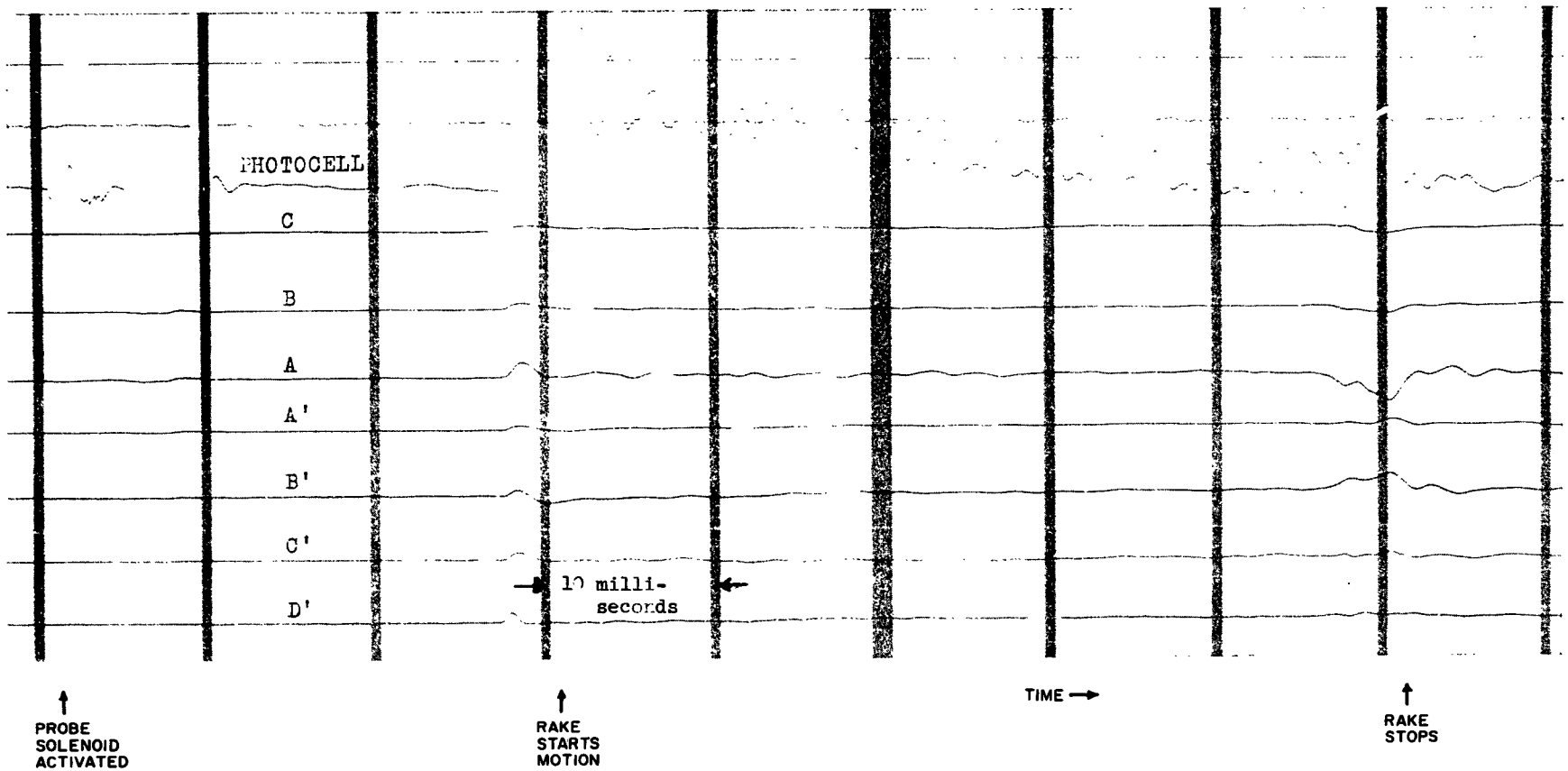

FIG. 12. PRESSURE AND POSITION TRACES — RUN A.

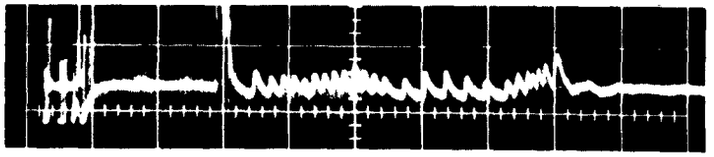

FIG. 13. OSCILLOSCOPE TRACE OF PHOTOCELL OUTPUT – RUN A.

TIME SCALE: 10 MILLISEC/CM.

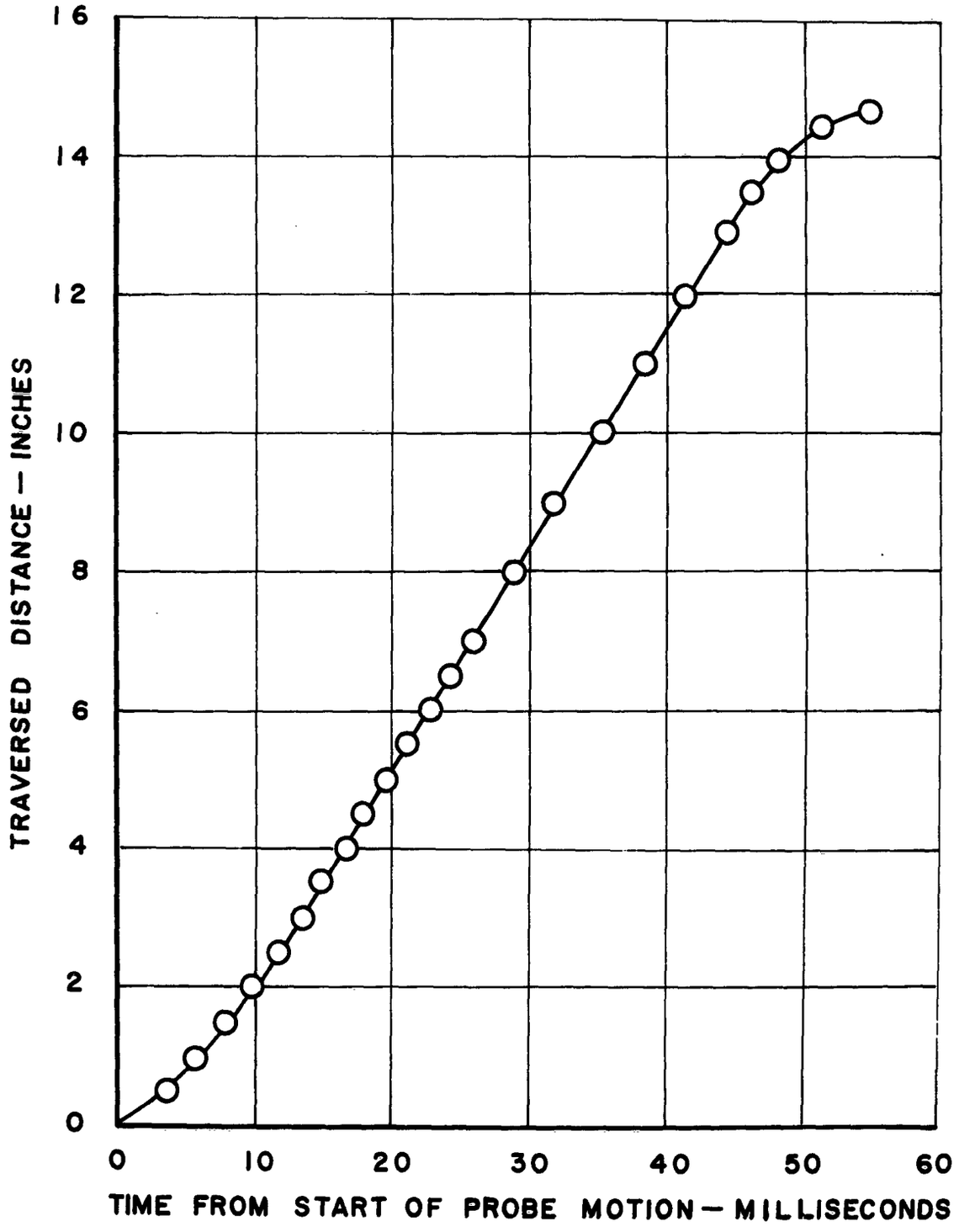

FIG. 14. TIME HISTORY OF POSITION OF PITOT-PRESSURE RAKE – RUN A.

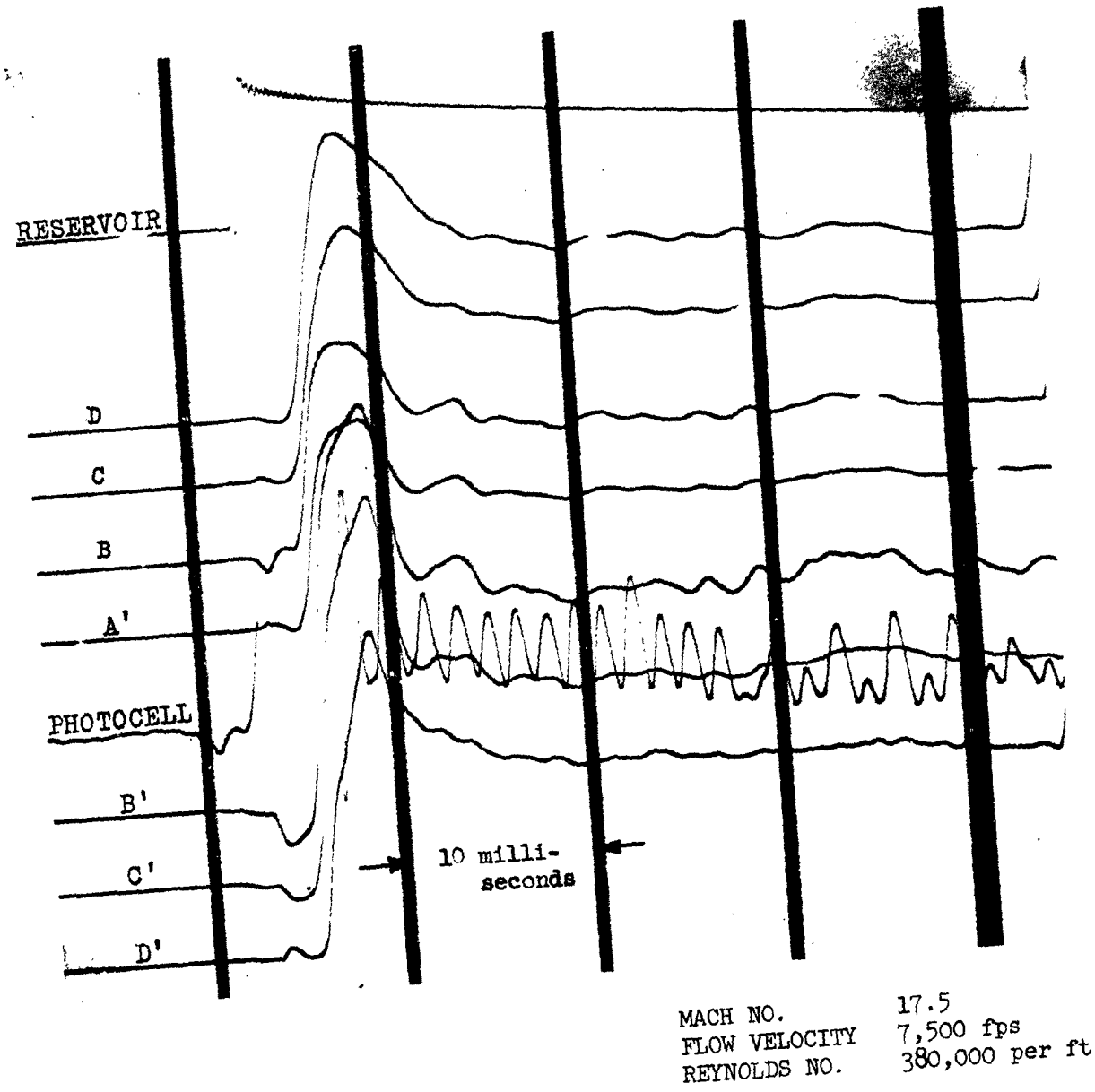

FIG. 15. PRESSURE AND POSITION TRACES – RUN B.

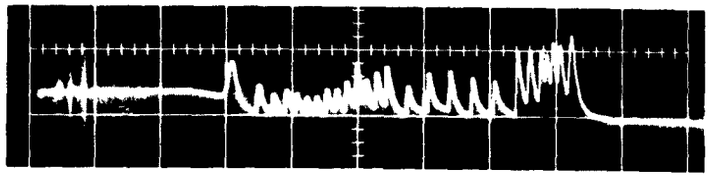

FIG. 16. OSCILLOSCOPE TRACE OF PHOTOCELL OUTPUT – RUN B.
TIME SCALE: 10 MILLISEC/CM.

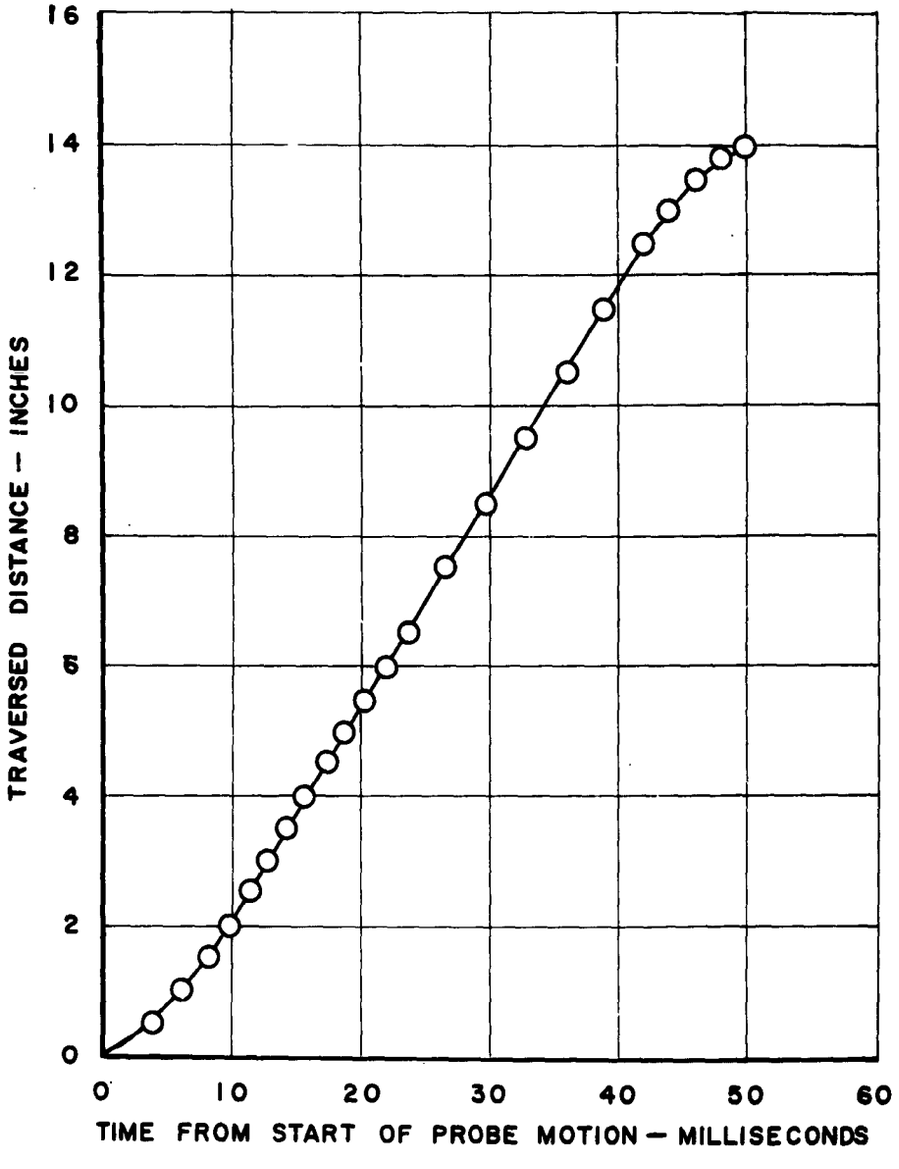

FIG. 17. TIME HISTORY OF POSITION OF PITOT-PRESSURE RAKE – RUN B.

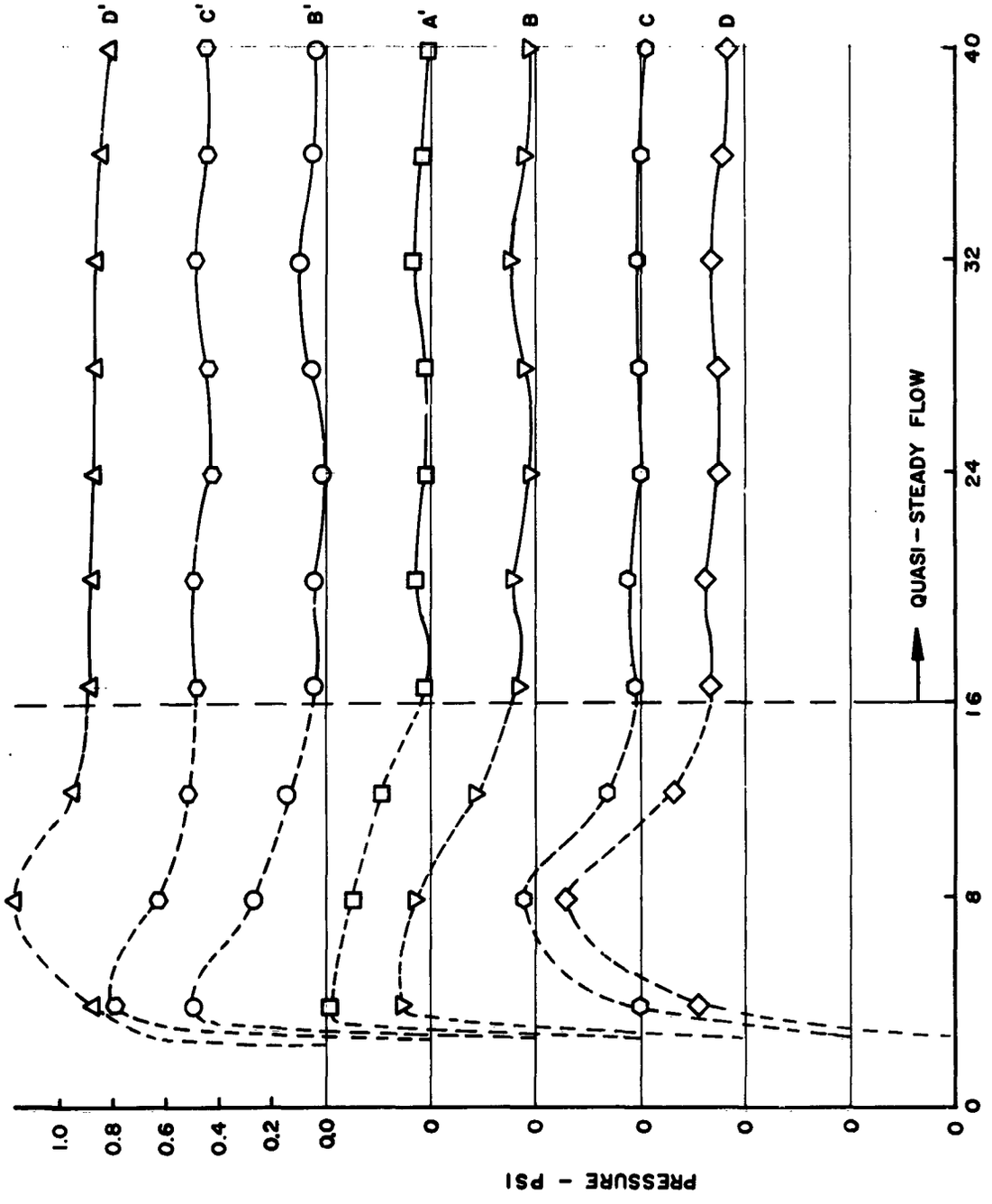

FIG. 18. PITOT PRESSURE - RUN B.

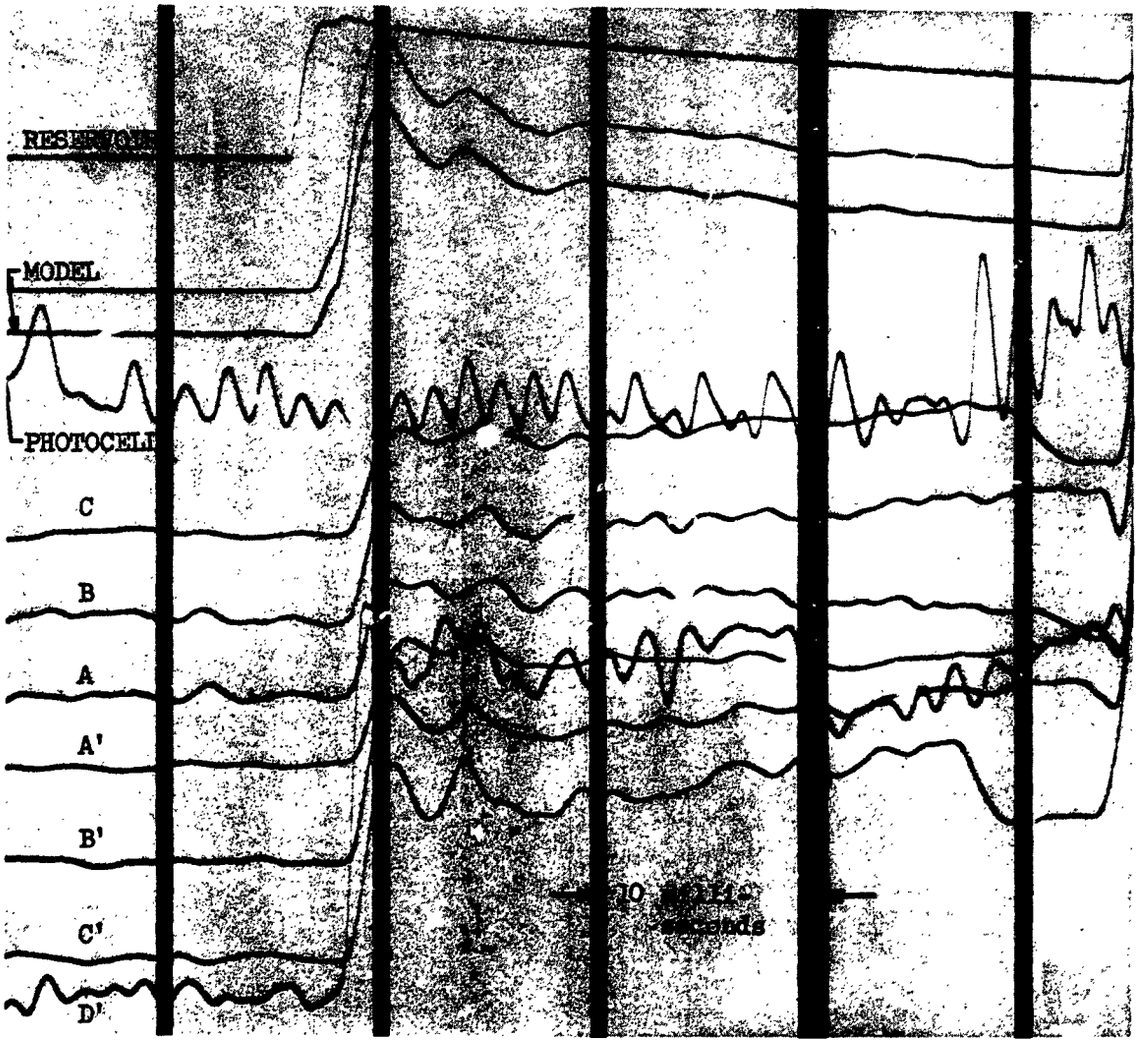

MACH NO.	17.5
FLOW VELOCITY	7,500 fps
REYNOLDS NO.	520,000 per ft

FIG. 19. PRESSURE AND POSITION TRACES – RUN C.

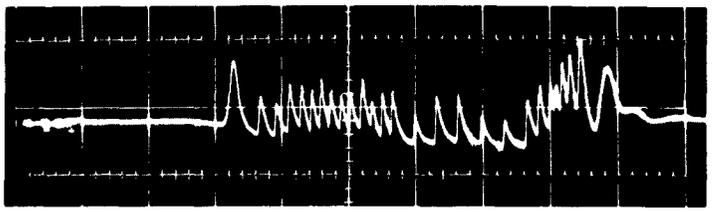

FIG. 20. OSCILLOSCOPE TRACE OF PHOTOCELL OUTPUT – RUN C.

TIME SCALE: 10 MILLISEC/CM.

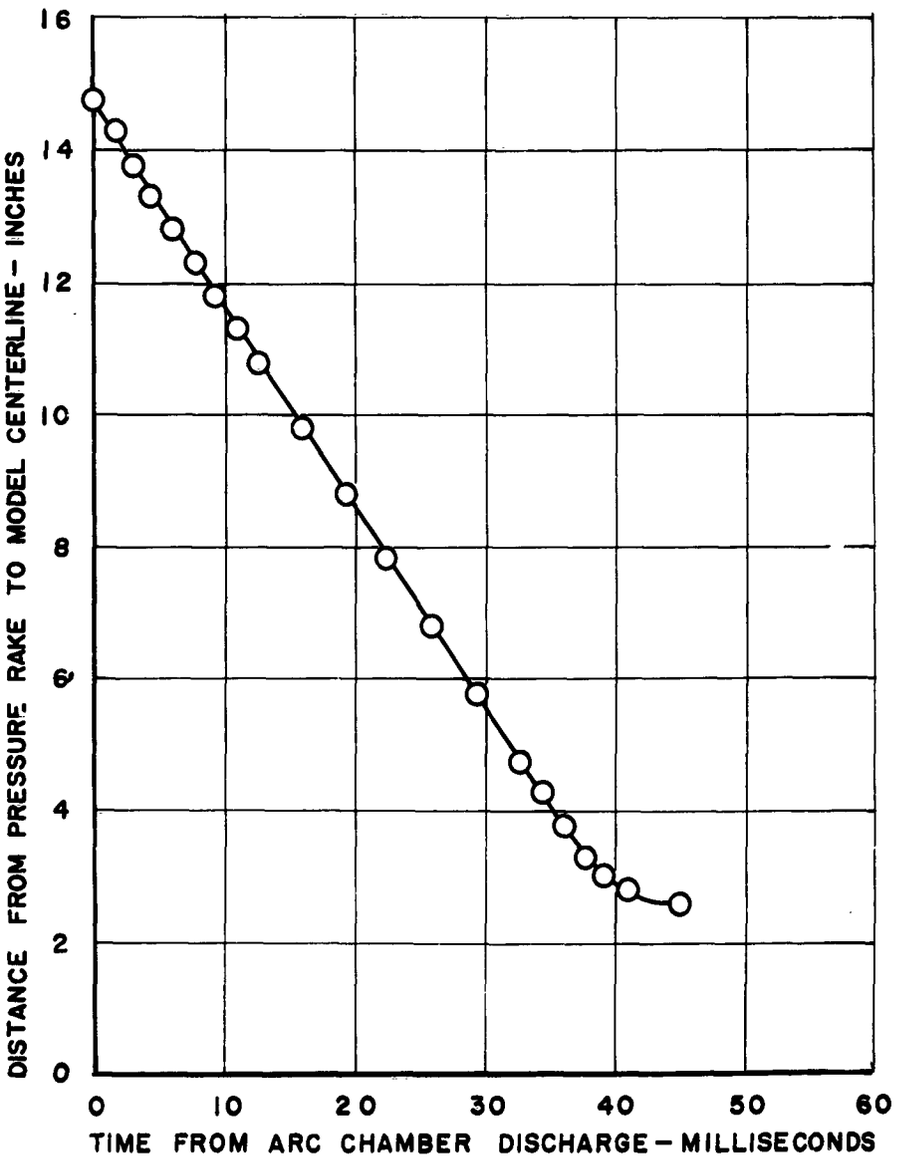

FIG. 21. TIME HISTORY OF POSITION OF PITOT-PRESSURE RAKE – RUN C.

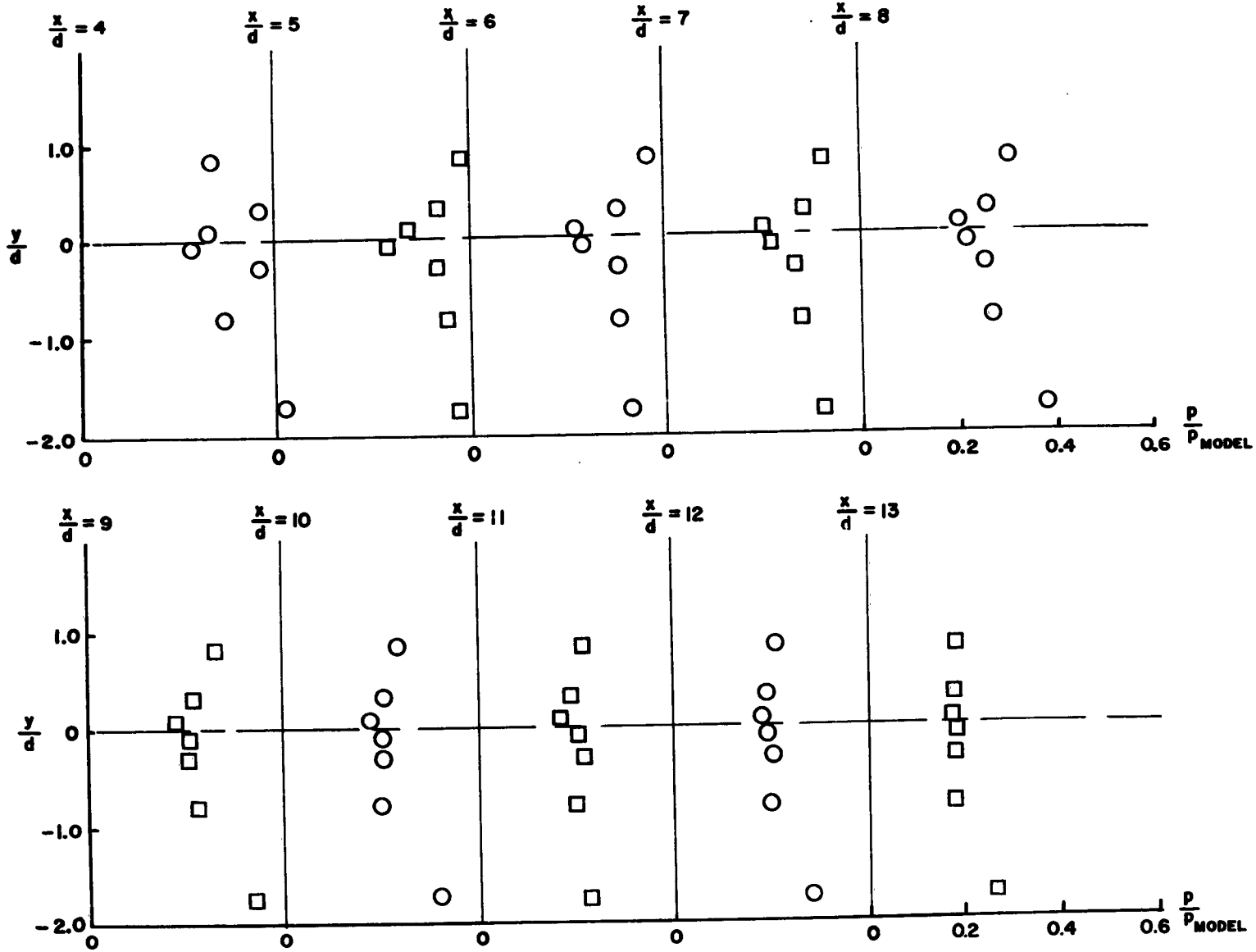

FIG. 22. PITOT-PRESSURE PROFILES – RUN C.